Probabilistic Engineering Mechanics 78 (2024) 103696

Contents lists available at ScienceDirect

Probabilistic Engineering Mechanics

journal homepage: www.elsevier.com/locate/probengmech

Fractional-order filter approximations for efficient stochastic response determination of wind-excited linear structural systems

Luca Roncallo [a,*], Ilias Mavromatis [b], Ioannis A. Kougioumtzoglou [b], Federica Tubino [a]

[a] Department of Civil, Chemical and Environmental Engineering (DICCA), Polytechnic School, University of Genoa, Via Montallegro 1, 16145, Genoa, Italy
[b] Department of Civil Engineering and Engineering Mechanics, Columbia University, 500 W 120th St, New York, NY, 10027, United States

ARTICLE INFO

Keywords:
Wind engineering
Stochastic dynamics
Fractional derivative
Filter approximation
Random vibration integral

ABSTRACT

A fractional-order filter approximation is developed for a wind turbulence stochastic excitation model. Specifically, the unknown filter parameters are determined by minimizing the error in the frequency domain between the original and the approximate power spectral densities. It is shown that compared to the limiting case of a standard integer-order filter, and for the same number of parameters to be optimized, the determined fractional-order filter with derivative elements of rational order yields enhanced accuracy. Further, the developed filter approximation enables the analytical calculation of stationary response moments of linear structural systems at practically zero computational cost. This is done by employing a complex modal analysis treatment of the filter state-variable equations, and by relying on Cauchy's residue theorem for evaluating analytically the related random vibration integrals. Comparisons with estimates based on Monte Carlo simulation data demonstrate a quite high degree of accuracy.

1. Introduction

Uncertainty modeling in the field of stochastic structural dynamics precedes the challenge of uncertainty propagation, and relates to the development of methodologies for analyzing measured data and for estimating pertinent stochastic models (e.g., Refs. [1–3]). In this regard, a wide range of excitations acting on structural systems are modeled, realistically, as stochastic processes. Depending on the quality and quantity of the available data, information about the underlying vector stochastic process is provided, typically, in the form of a power spectral density (PSD) matrix that shows, loosely speaking, the distribution of the process second-order statistics over the frequency domain.

Further, addressing the challenge of uncertainty propagation relates to solving stochastic differential equations governing the structural system dynamics; see Refs. [4–9] for a broad perspective on various solution techniques that have been developed in the field of stochastic structural dynamics over the past six decades. Notably, a common denominator in the aforementioned solution techniques is the role of the excitation process PSD as the input in the uncertainty propagation problem. Representatively, purely numerical solution schemes based on Monte Carlo simulation (MCS) rely on the development of methodologies for producing realizations compatible with the excitation PSD (e.g., Refs. [10,11]). Moreover, for linear systems, an analytical solution treatment is possible, first, by relying on a pivotal, closed-form, input-output relationship between the excitation and the response PSD, and second, by integrating the response PSD for determining response statistical moments (e.g., Refs. [6,12–14]).

It can be readily seen that the form of the input/excitation PSD, as estimated based on experimental data, affects significantly the accuracy degree and the computational efficiency exhibited by the solution techniques. In this regard, various modifications and/or approximations of the input PSD have been employed for reducing the overall cost associated with the uncertainty propagation problem. For example, as shown in Ref. [15], a minor modification in a popular model of auto-correlation function (defined as the inverse Fourier transform of the PSD) yields enhanced efficiency in the spectral representation of the underlying process via the Karhunen-Loeve expansion. This is of significant importance to a certain class of stochastic finite element solution techniques (e.g., Ref. [16]). Also, as shown in Ref. [17], due to certain mathematical peculiarities in its form, the Pierson-Moskowitz sea wave PSD needs to be slightly modified to be used within an efficient MCS solution scheme based on an auto-regressive model representation.

Further, filter approximations of the input/excitation PSD have been

* Corresponding author.
E-mail address: luca.roncallo@edu.unige.it (L. Roncallo).

https://doi.org/10.1016/j.probengmech.2024.103696
Received 3 June 2024; Received in revised form 21 August 2024; Accepted 19 September 2024
Available online 25 September 2024

catalytic for enhancing the versatility of various solution techniques (e.g., Refs. [18,19]). Indeed, modeling a general, non-white, excitation process as the output of a filter subjected to white noise input enables casting the governing equation of motion into an equivalent form exhibiting Markovian response. This equivalent form is of reduced mathematical complexity compared to the original one, and thus, can be handled by well-established solution techniques more easily. As a result, extensions of a wide range of solution techniques to treat non-white excitation processes are possible, in a straightforward manner, without any modifications of their original formulation. Of course, this is done at the expense of considering additional state variables and auxiliary equations. In passing, note that, in a similar manner, filter approximations of the system have also benefited considerably the efficient calculation of response statistics (e.g., Refs. [20–22]).

Furthermore, evaluating analytically random vibration integrals for determining statistical moments corresponding to the response of linear systems has been a persistent challenge in the field of stochastic structural dynamics (e.g., Refs. [14,23–25]). In this regard, a filter approximation treatment of the input/excitation PSD has been employed, routinely, for rendering the related integrands amenable to analytical integration based, for instance, on Cauchy's residue theorem (e.g., Ref. [26]), or on a spectral moments equations approach (e.g., Ref. [27]). Representatively, several filter approximations with varying degrees of accuracy have been proposed in Ref. [28] and in Ref. [27] for treating wave and wind excitations, respectively. Accordingly, the response statistical moments have been obtained analytically at practically zero computational cost.

Note, however, that the aforementioned efforts refer to approximations of the excitation PSD based on filters with integer-order derivatives. In fact, focusing on the field of wind engineering, the vast majority of the developed approximate/analytical solution methodologies rely on ordinary calculus concepts and tools (e.g., Refs. [29–33]). In this context, it has been shown that fractional calculus, which can be construed as a generalization of ordinary calculus, provides enhanced modeling capabilities (e.g., Refs. [34–36]). Indeed, as a representative example, the celebrated Kanai-Tajimi excitation PSD in earthquake engineering was recently generalized in Ref. [37] by considering fractional-order derivatives in the model. It was further shown that this alternative PSD model that is, in essence, a fractional-order filter to white noise input, exhibits certain advantages compared to the standard model, such as a more realistic representation of the soil viscoelastic behavior.

In this paper, a fractional-order filter approximation is developed for the wind turbulence stochastic excitation model proposed in Ref. [38]. Specifically, the unknown filter parameters are determined by minimizing the error in the frequency domain between the original and the approximate PSDs. It is shown that compared to the limiting case of a standard integer-order filter, and for the same number of parameters to be optimized, the determined fractional-order filter with derivative elements of rational order yields enhanced accuracy. Further, the developed filter approximation enables the analytical calculation of stationary response moments of linear structural systems at practically zero computational cost. This is done by employing a complex modal analysis treatment of the filter state-variable equations, and by relying on Cauchy's residue theorem for evaluating analytically the related random vibration integrals. Comparisons with estimates based on MCS data demonstrate a quite high degree of accuracy. Notably, a significant advantage of the technique relates to the fact that the exhibited accuracy degree for determining system response statistics can be controlled by the analyst by considering, representatively, higher-order filter approximations of the input turbulence model.

2. Preliminaries

Consider the wind speed recorded at a point in space associated with a synoptic event, such as tropical and extra-tropical cyclones. The recorded wind speed $v(t)$ can be approximated with reasonable accuracy as a stationary Gaussian process [39]. Further, it can be decomposed into a mean and a fluctuating parts as

$$v(t) = \bar{v} + \upsilon(t) \tag{1}$$

where $\bar{v}$ is the mean wind speed and $\upsilon(t)$ represents the alongwind turbulent fluctuation modeled as a zero-mean stationary Gaussian process with standard deviation σ_υ. Note that various models have been proposed in the literature for the PSD corresponding to $\upsilon(t)$ [40]. Representatively, and without loss of generality in the ensuing analysis, a quite popular model in wind engineering relates to the, normalized by σ_υ^2, one-sided PSD [38]

$$\frac{\omega S_\upsilon(\omega)}{\sigma_\upsilon^2} = \frac{1}{2\pi} \frac{d_\upsilon \omega L_\upsilon/\bar{v}}{\left[1 + 1.5\frac{d_\upsilon L_\upsilon}{2\pi\bar{v}}\omega\right]^{5/3}} \tag{2}$$

where L_υ is the integral length scale of the turbulence that depends on the height above the terrain, $d_\upsilon = 6.868$ is a constant associated with the horizontal component of the wind velocity, and ω is the circular frequency.

Next, consider a stochastically excited linear Single-Degree-Of-Freedom (SDOF) oscillator whose equation of motion is given by

$$\ddot{x}(t) + 2\xi\omega_0\dot{x}(t) + \omega_0^2 x(t) = \frac{1}{m} f(t) \tag{3}$$

In Eq. (3), m denotes the mass, ω_0 represents the natural frequency, and ξ is the damping ratio. Considering next relatively small values of $\upsilon(t)$ compared to the mean velocity $\bar{v}$, $f(t)$ is given by [41]

$$f(t) = \rho A c_D \bar{v} \upsilon(t) \tag{4}$$

In Eq. (4), ρ is the air density, A is the surface of the oscillator normal to the wind velocity, and c_D is the corresponding drag coefficient. Based on Eq. (4), the PSD of $f(t)$ takes the form

$$S_f(\omega) = (\rho A c_D \bar{v})^2 S_\upsilon(\omega) \tag{5}$$

Further, the oscillator stationary response PSD is given by the celebrated input-output (excitation-response) spectral relationship of the linear random vibration theory (e.g., Ref. [6]); that is,

$$S_x(\omega) = (\rho A c_D \bar{v})^2 |H(\omega)|^2 S_\upsilon(\omega) \tag{6}$$

where the frequency response function $H(\omega)$ takes the form

$$H(\omega) = \frac{1}{m} \frac{1}{\omega_0^2 - \omega^2 + 2i\xi\omega_0\omega} \tag{7}$$

Notably, a significant advantage of the algebraic Eq. (6) relates to the fact that the oscillator stationary response variance can be obtained by simply integrating the response PSD over the frequency domain, i.e.,

$$\sigma_x^2 = \int_0^{+\infty} S_x(\omega) d\omega \tag{8}$$

3. Fractional-order filter approximation of the wind turbulence spectrum

Note that, due to the form of $S_\upsilon(\omega)$ given by Eq. (2), the analytical evaluation of the integral of Eq. (8) is a rather daunting, if not impossible, task. More generally, evaluating analytically random vibration integrals for determining statistical moments corresponding to the response of linear structural systems has been a persistent challenge in the field of stochastic structural dynamics [6]. In this regard, one of the most versatile approaches for circumventing this challenge relates to a filter approximation treatment of the excitation process. Succinctly stated, the rationale relates to representing the excitation process as the

output of a dynamic system (filter) subjected to a white noise input. In this manner, the numerical computation of the relevant integrals can be replaced by analytical integration based, for instance, on Cauchy's residue theorem (e.g. Ref. [26]), or on a spectral moments equations approach [12]. Representatively, several filter approximations with varying degrees of accuracy have been proposed in Ref. [28] and in Ref. [27] for treating wave and wind excitations, respectively. Accordingly, closed form expressions for the response moments have been obtained at zero computational cost. This is particularly important for higher-dimensional Multi-Degree-Of-Freedom (MDOF) systems for which the cost associated with the numerical calculation of the response moments becomes non-trivial (e.g., Refs. [22,27]).

However, note that the aforementioned research efforts rely on ordinary calculus and employ time-domain filters with integer-order derivatives. In this regard, it can be argued that an alternative modeling that utilizes filters with non-integer-order derivatives exhibits certain advantages compared to the standard approach. Indeed, fractional calculus can be construed as a generalization of ordinary calculus, and as such provides with enhanced modeling capabilities [34–36]. In fact, considering the same number of unknowns in the filter approximation of Eq. (2), it is shown herein that a fractional-order filter with derivative elements of rational order yields improved accuracy compared to a related integer-order filter. Notably, the latter can be viewed as a limiting case of the former.

Specifically, the wind fluctuating component $v(t)$ is represented as the response of a linear dynamic system (filter) with fractional derivative terms under white noise excitation. In particular, the filter equation takes the form

$$p\left(d_v\frac{L_v}{\bar{v}}\right)^2\ddot{v}(t)+q\left(d_v\frac{L_v}{\bar{v}}\right)^\beta\left({}_CD_0^\beta v\right)(t)+rv(t)=w(t) \tag{9}$$

Where $w(t)$ is a white noise stochastic process with constant PSD S_0, p, q and r denote real coefficients to be identified, ${}_CD_0^\beta$ is the Caputo fractional derivative of order $\beta\in(0,1]$ given by

$$\left({}_CD_0^\beta v\right)(t)=\frac{1}{\Gamma(1-\beta)}\int_0^t(t-\tau)^{-\beta}\dot{v}(\tau)d\tau \tag{10}$$

with $\Gamma(z)$ the gamma function defined as

$$\Gamma(z)=\int_0^{+\infty}t^{z-1}e^{-t}dt \tag{11}$$

In passing, note that for the limiting case $\beta=1$ the Caputo fractional derivative in Eq. (9) degenerates to an ordinary derivative, i.e., $\left({}_CD_0^\beta v\right)(t)=\dot{v}(t)$, and the filter becomes of integer order. Further, the frequency response function corresponding to Eq. (9) takes the form

$$H_f(\omega)=\frac{1}{p\left(d_v\frac{L_v}{\bar{v}}\right)^2(i\omega)^2+q\left(d_v\frac{L_v}{\bar{v}}\right)^\beta(i\omega)^\beta+r} \tag{12}$$

Thus, the PSD of the wind fluctuating component $v(t)$ is expressed as

$$S_v(\omega)=\left|H_f(\omega)\right|^2S_0 \tag{13}$$

Next, substituting Eq. (13) into Eq. (6) yields the oscillator response PSD

$$S_x(\omega)=(\rho Ac_D\bar{v})^2|H(\omega)|^2\left|H_f(\omega)\right|^2S_0 \tag{14}$$

Further, substituting Eq. (14) into Eq. (8), the oscillator stationary response variance is expressed as

$$\sigma_x^2=(\rho Ac_D\bar{v})^2S_0\int_0^{+\infty}|H(\omega)|^2\left|H_f(\omega)\right|^2d\omega \tag{15}$$

Clearly, the proposed filter approximation treatment requires the identification of the parameters p, q, r, β and S_0 in Eq. (9). Regarding the excitation PSD constant value S_0 , considering Eqs. (2), (12) and (13) yields

$$S_0=\frac{1}{2\pi}\frac{\sigma_v^2d_vL_v}{\bar{v}} \tag{16}$$

In the following sections 3.1 and 3.2, integer- and fractional-order filters are determined, respectively. In this regard, the fractional derivative order β is set either equal to 1 (integer-order filter), or equal to 5/6 (fractional-order filter) so that terms with powers 5/3 appear in the frequency domain, as is the case with the denominator of the original Eq. (2). Further, the parameters p, q and r are determined by employing a numerical optimization scheme [42], and by minimizing the error between Eqs. (2) and (13). Note that caution should be exercised to ensure that the identified model of Eq. (13) (or, equivalently, of Eq. (9)) represents a stable system in the bound-input-bound-output sense (e.g., Ref. [43]). Otherwise, utilizing Eq. (9) for performing time-domain response analyses within an MCS context does not warrant stability in the sense of the system reaching stationarity from a quiescent initial state. In this context, an extended Routh-Hurwitz criterion [44] is employed in the numerical example of section 5.1 for examining the stability of the identified fractional-order model governed by Eq. (9).

3.1. Integer-order filter approximation

It is readily seen that for the limiting case $\beta=1$ Eq. (9) degenerates to a standard linear second-order stochastic differential equation; that is,

$$p\left(d_v\frac{L_v}{\bar{v}}\right)^2\ddot{v}(t)+q\left(d_v\frac{L_v}{\bar{v}}\right)\dot{v}(t)+rv(t)=w(t) \tag{17}$$

Accordingly, the frequency response function of Eq. (12) becomes

$$H_{f,1}(\omega)=\frac{1}{p\left(d_v\frac{L_v}{\bar{v}}\right)^2(i\omega)^2+q\left(d_v\frac{L_v}{\bar{v}}\right)(i\omega)+r} \tag{18}$$

In general, this kind of integer-order filter approximation has been widely used in various diverse applications in engineering dynamics (e.g., Refs. [19,22,27,28,45]). Notably, depending on the desired degree of accuracy, higher-order filter approximations can be readily accounted for within the same framework at the expense, of course, of additional computational cost related to the augmented vector of unknown coefficients (e.g., Refs. [22,28]).

3.2. Fractional-order filter approximation

As noted previously, for the general case of a fractional-order derivative with $\beta\in(0,1)$, the form of Eq. (2) serves as a guide for selecting the value of β in an a priori manner. In this regard, the value $\beta=5/6$ is employed so that terms with powers 5/3 appear in the filter approximation in the frequency domain; thus, matching the power 5/3 in the denominator of the original Eq. (2). In this regard, Eq. (9) becomes

$$p\left(d_v\frac{L_v}{\bar{v}}\right)^2\ddot{v}(t)+q\left(d_v\frac{L_v}{\bar{v}}\right)^{5/6}\left({}_CD_0^{5/6}v\right)(t)+rv(t)=w(t) \tag{19}$$

and Eq. (12) takes the form

$$H_f(\omega)=\frac{1}{p\left(d_v\frac{L_v}{\bar{v}}\right)^2(i\omega)^2+q\left(d_v\frac{L_v}{\bar{v}}\right)^{5/6}(i\omega)^{5/6}+r} \tag{20}$$

Obviously, setting $\beta = 5/6$ also has the advantage of reducing the number of unknowns to be identified by the numerical optimization scheme. Alternatively, β can be treated as an additional free variable to be identified.

4. Advantages of the filter approximation for determining oscillator response statistics

In this section it is shown that the filter approximation proposed in Eq. (9) enables the analytical derivation of closed-form expressions for the linear oscillator response variance. In this regard, the stationary response variance given by Eq. (8) is determined at practically zero computational cost. This is done by employing a spectral moments equations approach (e.g., Refs. [6,12]) for the case of integer-order filter, and by resorting to Cauchy's residue theorem (e.g., Refs. [25,26]) for the case of fractional-order filter.

4.1. Integer-order filter approximation

For the case of integer-order filter, Eq. (15) becomes

$$\sigma_x^2 = (\rho A c_D \bar{v})^2 S_0 \int_0^{+\infty} |H(\omega)|^2 |H_{f,I}(\omega)|^2 d\omega \tag{21}$$

Considering Eqs. (7) and (18), Eq. (21) is cast, equivalently, in the form

$$\sigma_x^2 = (\rho A c_D \bar{v})^2 S_0 I_4 \tag{22}$$

where

$$I_4 = \frac{1}{2} \int_{-\infty}^{+\infty} \frac{1}{\Lambda_4(i\omega)\Lambda_4(-i\omega)} d\omega \tag{23}$$

and

$$\Lambda_4(i\omega) = \frac{1}{m}\left[\delta_4 (i\omega)^4 + \delta_3 (i\omega)^3 + \delta_2 (i\omega)^2 + \delta_1 (i\omega) + \delta_0\right] \tag{24}$$

with

$$\delta_4 = p\left(d_v \frac{L_v}{\bar{v}}\right)^2 \tag{25}$$

$$\delta_3 = 2\xi\omega_0 p\left(d_v \frac{L_v}{\bar{v}}\right)^2 + q\left(d_v \frac{L_v}{\bar{v}}\right) \tag{26}$$

$$\delta_2 = p\left(d_v \frac{L_v}{\bar{v}}\right)^2 \omega_0^2 + 2\xi\omega_0 q\left(d_v \frac{L_v}{\bar{v}}\right) + r \tag{27}$$

$$\delta_1 = q\left(d_v \frac{L_v}{\bar{v}}\right)\omega_0^2 + 2\xi\omega_0 r \tag{28}$$

$$\delta_0 = r\omega_0^2 \tag{29}$$

Next, following a standard spectral moments equations approach [6,12], the integral of Eq. (23) can be evaluated analytically as

$$I_4 = \frac{\pi}{2\delta_4} \frac{|\Theta_1|}{|\Theta_0|} \tag{30}$$

where

$$\Theta_1 = \begin{pmatrix} 0 & 0 & 0 & 1 \\ -\delta_4 & \delta_2 & -\delta_0 & 0 \\ 0 & -\delta_3 & \delta_1 & 0 \\ 0 & \delta_4 & -\delta_2 & \delta_0 \end{pmatrix} \tag{31}$$

$$\Theta_0 = \begin{pmatrix} \delta_3 & -\delta_1 & 0 & 0 \\ -\delta_4 & \delta_2 & -\delta_0 & 0 \\ 0 & -\delta_3 & \delta_1 & 0 \\ 0 & \delta_4 & -\delta_2 & \delta_0 \end{pmatrix} \tag{32}$$

Further, combining Eq. (22) and (30)-(32) yields

$$\sigma_x^2 = \frac{d_v L_v \bar{v} (\rho A c_D \sigma_v)^2}{4\xi m^2 \omega_0^3 qr} \Omega(p, q, r, d_v, L_v, \bar{v}, \xi, \omega_0) \tag{33}$$

where Ω is a function of the parameters $p, q, r, d_v, L_v, \bar{v}, \xi, \omega_0$ given by

$$\Omega = \frac{qr + 2\xi d_v \frac{L_v}{\bar{v}} \omega_0 \left[q^2 + \left(d_v \frac{L_v}{\bar{v}}\right)^2 \omega_0^2 p^2\right] + 4\xi^2 \left(d_v \frac{L_v}{\bar{v}}\right)^2 \omega_0^2 pq}{\left(d_v \frac{L_v}{\bar{v}}\right)^2 \omega_0^2 q^2 + \left[r - \left(d_v \frac{L_v}{\bar{v}}\right)^2 \omega_0^2 p\right]^2 + 2\xi d_v \frac{L_v}{\bar{v}} \omega_0 q \left[r + \left(d_v \frac{L_v}{\bar{v}}\right)^2 \omega_0^2 p\right] + 4\xi^2 \left(d_v \frac{L_v}{\bar{v}}\right)^2 \omega_0^2 pr} \tag{34}$$

Clearly, due to the integer-order filter approximation of Eq. (17), the oscillator stationary response variance given by Eq. (33) has been derived in closed form, at zero computational cost. Also, note that the analytical calculation of the integral in Eq. (8) is exact, and the only source of error relates to the input (excitation PSD) modeling.

4.2. Fractional-order filter approximation

For the fractional-order filter, a state-variable formulation of Eq. (19) is employed in conjunction with a complex modal analysis for decoupling the resulting system of equations (e.g., Refs. [46–48]). Notably, the eigenvalues corresponding to the complex modal analysis treatment are determined herein, analytically, based on an approximate solution approach; see also [49] for a somewhat similar solution treatment based on perturbation theory. Next, applying Cauchy's residue theorem (e.g., Ref. [25]), a closed-form expression is derived for the oscillator stationary response variance given by Eq. (8).

Specifically, Eq. (19) is recast, equivalently, in the form [47,48]

$$\sum_{j=1}^{n} c_j \left({}_C D_0^{j/b} v\right)(t) + v(t) = w(t) \tag{35}$$

where $\beta = a/b$, $a = 5$, $b = 6$, $n = 2b$ and $c_j = 0 \ \forall j \neq a, n$ with $c_5 = q\left(d_v \frac{L_v}{\bar{v}}\right)^{5/6}$ and $c_{12} = p\left(d_v \frac{L_v}{\bar{v}}\right)^2$. Next, considering the state-variable vector

$$\mathbf{z}^T(t) = \left[v(t) \ \left({}_CD_0^{1/b}v\right)(t) \ \left({}_CD_0^{2/b}v\right)(t) \ \ldots \ \left({}_CD_0^{(n-1)/b}v\right)(t)\right] \tag{36}$$

Eq. (35) becomes

$$\mathbf{A}\left({}_CD_0^{1/b}\mathbf{z}\right)(t) + \mathbf{B}\mathbf{z}(t) = \mathbf{g}(t) \tag{37}$$

where

$$\begin{aligned}\mathbf{A} &= \begin{bmatrix} c_1 & c_2 & \cdots & c_{n-1} & c_n \\ c_2 & c_3 & \cdots & c_n & 0 \\ \vdots & \vdots & \ddots & \vdots & \vdots \\ c_{n-1} & c_n & \cdots & 0 & 0 \\ c_n & 0 & \cdots & 0 & 0 \end{bmatrix}, \mathbf{B} \\ &= \begin{bmatrix} r & 0 & \cdots & 0 & 0 \\ 0 & -c_2 & \cdots & -c_{n-1} & -c_n \\ \vdots & \vdots & \ddots & \vdots & \vdots \\ 0 & -c_{n-1} & \cdots & 0 & 0 \\ 0 & -c_n & \cdots & 0 & 0 \end{bmatrix}, \text{and } \mathbf{g}^T(t) = [w(t) \ 0 \ \ldots \ 0]\end{aligned} \tag{38}$$

Further, to decouple the system of equations shown in Eq. (37), an eigenvalue analysis of the matrix

$$\mathbf{D} = \mathbf{A}^{-1}\mathbf{B} = \frac{1}{c_n}\begin{bmatrix} 0 & -c_n & \cdots & 0 & 0 \\ 0 & 0 & \cdots & 0 & 0 \\ \vdots & \vdots & \ddots & \vdots & \vdots \\ 0 & 0 & \cdots & 0 & -c_n \\ r & c_1 & \cdots & c_{n-2} & c_{n-1} \end{bmatrix} \tag{39}$$

yields the eigenvectors matrix $\mathbf{\Psi}$. Next, employing the complex modal transformation

$$\mathbf{z}(t) = \Psi\mathbf{p}(t) \tag{40}$$

substituting Eq. (40) into Eq. (37), and pre-multiplying by $\mathbf{\Psi}^T$, leads to

$$\mathbf{U_d}\left({}_CD_0^{1/b}\mathbf{p}\right)(t) + \mathbf{V_d}\mathbf{p}(t) = \widetilde{\mathbf{g}}(t) \tag{41}$$

In Eq. (41), $\widetilde{\mathbf{g}}(t) = \mathbf{\Psi}^T\mathbf{g}(t)$, and $\mathbf{U_d}$, $\mathbf{V_d}$ are diagonal matrixes given by

$$\mathbf{U_d} = \mathbf{\Psi}^T\mathbf{A}\mathbf{\Psi} \tag{42}$$

$$\mathbf{V_d} = \mathbf{\Psi}^T\mathbf{B}\mathbf{\Psi} \tag{43}$$

with μ_j and ς_j denoting the elements in the diagonals of $\mathbf{U_d}$ and $\mathbf{V_d}$, respectively. Clearly, Eq. (41) is an uncoupled system of n modal equations, where the j-th equation takes the form

$$\left({}_CD_0^{1/b}p_j\right)(t) + \lambda_j p_j(t) = \varepsilon_{1j}w(t) \quad j = 1, \ldots, n \tag{44}$$

In Eq. (44), $\lambda_j = \varsigma_j/\mu_j$ are the eigenvalues of $\mathbf{D}$, and $\varepsilon_{1j} = \psi_{1j}/\mu_j$. In this regard, the solution of Eq. (35) can be expressed as

$$v(t) = z_1(t) = \sum_{j=1}^{n}\psi_{1j}p_j(t) \tag{45}$$

and the PSD of the stationary process $v(t)$ is given by [6,47]

$$S_v(\omega) = S_0\sum_{j=1}^{n}\sum_{k=1}^{n}\psi_{1j}^*\psi_{1k}S_{p_jp_k}(\omega) \tag{46}$$

where

$$S_{p_jp_k}(\omega) = \frac{\varepsilon_{1j}^*\varepsilon_{1k}}{\left(\sqrt[b]{-i\omega} + \lambda_j^*\right)\left(\sqrt[b]{i\omega} + \lambda_k\right)} \tag{47}$$

Thus, substituting Eq. (46) into Eq. (6) yields

$$S_x(\omega) = (\rho A c_D \bar{v})^2 S_0 |H(\omega)|^2 \sum_{j=1}^{n}\sum_{k=1}^{n}\frac{\psi_{1j}^*\psi_{1k}\varepsilon_{1j}^*\varepsilon_{1k}}{\left(\sqrt[b]{-i\omega} + \lambda_j^*\right)\left(\sqrt[b]{i\omega} + \lambda_k\right)} \tag{48}$$

Obviously, the eigenvalue problem pertaining to matrix $\mathbf{D}$ in Eq. (39) can be readily solved numerically (e.g., Ref. [50]). However, it is shown in the ensuing analysis that, alternatively, an approximate analytical solution treatment of the eigenvalue problem yields a quite satisfactory degree of accuracy. The interested reader is also directed to Ref. [49] for a somewhat similar approximate solution treatment based on perturbation theory.

Specifically, the characteristic polynomial corresponding to matrix $\mathbf{D}$ takes the form

$$\frac{p}{r}\left(d_\nu\frac{L_\nu}{\bar{v}}\right)^2\lambda^{12} - \frac{q}{r}\left(d_\nu\frac{L_\nu}{\bar{v}}\right)^{5/6}\lambda^5 + 1 = 0 \tag{49}$$

or, equivalently,

$$\frac{p}{q}\left(d_\nu\frac{L_\nu}{\bar{v}}\right)^{7/6}\lambda^{12} - \lambda^5 + \frac{r}{q\left(d_\nu\frac{L_w}{\bar{v}}\right)^{5/6}} = 0 \tag{50}$$

Next, focusing on the coefficient multiplying λ^{12} in Eq. (50), it is shown in the numerical application of section 5.1 that the identified parameters p, q are related so that $p \ll q$, and in particular, $p \propto 10^{-4}$ and $q \propto 10^{-1}$. Further, typical values provided by relevant codes (e.g., Ref. [51]) for the term $L_\nu/\bar{v}$, which depends exclusively on wind speed properties, are within the range of 4 s–170 s. In fact, even smaller values correspond to the case of thunderstorms [52,53]. Thus, it is seen that the coefficient multiplying λ^{12} in Eq. (50) is, approximately, at least two orders of magnitude smaller than the unit coefficient multiplying λ^5. In this regard, based on the above rationale, the first term in Eq. (50) is neglected, and the characteristic polynomial is approximated by

$$\lambda^5 - \frac{r}{q\left(d_\nu\frac{L_w}{\bar{v}}\right)^{5/6}} = 0 \tag{51}$$

Notably, Eq. (51) can be readily solved analytically. Specifically, considering a solution in the general complex polar form

$$\lambda = |\lambda|e^{i\vartheta} \tag{52}$$

substituting into Eq. (51), and manipulating, yields

$$|\lambda| = \left(\frac{\bar{v}}{d_\nu L_\nu}\right)^{1/6}\left(\frac{r}{q}\right)^{1/5} \tag{53}$$

and

$$\vartheta = k\frac{2\pi}{5} \quad k = 1, \ldots, 5 \tag{54}$$

Thus, relying on an approximate analytical treatment, 5 eigenvalues (out of the original 12) associated with the characteristic polynomial of Eq. (50) have been determined in the closed form given by Eqs. (52)–(54). These eigenvalues are used in the ensuing analysis in Eqs. (46) and (47) for approximating the PSD of the stationary process $v(t)$ by truncating the summations accordingly. Note that the degree of accuracy exhibited by the proposed analytical solution treatment is assessed in section 5.1 by comparing the closed-form estimates of Eqs. (52)–(54) with the eigenvalues obtained by solving numerically the characteristic polynomial of Eq. (48). Further, the efficacy of the analytical estimates of Eqs. (52)–(54) to approximate the PSD of $v(t)$ via Eqs. (46) and (47) is demonstrated as well.

Overall, substituting the 5 eigenvalues of Eqs. (52)–(54) into Eq. (48), and thus, considering in the summations 5 out of the $n = 12$ terms, Eq. (15) yields the oscillator stationary response variance in the form

$$\sigma_x^2 = (\rho A c_D \bar{v})^2 S_0 \sum_{j=1}^{5}\sum_{k=1}^{5} \psi_{1j}^{*}\psi_{1k}\varepsilon_{1j}^{*}\varepsilon_{1k} I_{jk} \tag{55}$$

where

$$I_{jk} = \int_0^{+\infty} |H(\omega)|^2 \frac{d\omega}{\left(\sqrt[b]{-i\omega} + \lambda_j^{*}\right)\left(\sqrt[b]{i\omega} + \lambda_k\right)} \tag{56}$$

or, equivalently, by taking into account Eq. (7),

$$I_{jk} = \frac{1}{m^2}\int_0^{+\infty} \frac{d\omega}{\left[\left(\sqrt[b]{-i\omega} + \lambda_j^{*}\right)\left(\sqrt[b]{i\omega} + \lambda_k\right)\right]\left[\left(\omega_0^2 - \omega^2\right)^2 + \left(2\xi\omega_0\omega\right)^2\right]} \tag{57}$$

Next, the integral I_{jk} in Eq. (57) is calculated analytically based on Cauchy's residue theorem (e.g., Ref. [25]). In this regard, considering the change of variables $s = \sqrt[b]{\omega}$, Eq. (57) becomes

$$I_{jk} = \frac{1}{m^2}\int_0^{+\infty} \frac{bs^{b-1}}{\left(s + i^{-3/b}\lambda_j^{*}\right)\left(s + i^{-1/b}\lambda_k\right)\left(\omega_0^2 - s^{2b} + 2\xi\omega_0 s^b\right)\left(\omega_0^2 - s^{2b} - 2\xi\omega_0 s^b\right)} ds \tag{58}$$

Eq. (58) is written, equivalently, as

$$I_{jk} = \frac{b}{m^2}\int_0^{+\infty} f_{jk}(s) ds \tag{59}$$

where

$$f_{jk}(s) = \frac{s^{b-1}}{(s - s_{1,j})(s - s_{2,k})\Pi_{m=3}^{N}(s - s_m)} \tag{60}$$

Note that the $N = 4b + 2$ roots of the integrand function in Eq. (60) are given by

$$\begin{aligned}
s_{1,j} &= -i^{-3/b}\lambda_j^{*}\\
s_{2,k} &= -i^{-1/b}\lambda_k\\
s_3 &= (-1)^{2/b}\left(\omega_0\sqrt{1-\xi^2} - i\xi\omega_0\right)^{1/b}\\
s_4 &= (-1)^{4/b}\left(\omega_0\sqrt{1-\xi^2} - i\xi\omega_0\right)^{1/b}\\
s_5 &= -\left(\omega_0\sqrt{1-\xi^2} - i\xi\omega_0\right)^{1/b}\\
s_6 &= -s_3\\
s_7 &= -s_4\\
s_8 &= -s_5\\
s_9 &= (-1)^{2b}\left(-\omega_0\sqrt{1-\xi^2} - i\xi\omega_0\right)^{1/b}\\
s_{10} &= (-1)^{4/b}\left(-\omega_0\sqrt{1-\xi^2} - i\xi\omega_0\right)^{1/b}\\
s_{11} &= -\left(-\omega_0\sqrt{1-\xi^2} - i\xi\omega_0\right)^{1/b}\\
s_{12} &= -s_9\\
s_{13} &= -s_{10}\\
s_{14} &= -s_{11}\\
s_{15} &= i^{2/b}s_9\\
s_{16} &= i^{2/b}s_{10}\\
s_{17} &= i^{2/b}s_{11}\\
s_{18} &= -s_{15}\\
s_{19} &= -s_{16}\\
s_{20} &= -s_{17}\\
s_{21} &= i^{2/b}s_3\\
s_{22} &= i^{2/b}s_4\\
s_{23} &= i^{2/b}s_5\\
s_{24} &= -s_{21}\\
s_{25} &= -s_{22}\\
s_{26} &= -s_{23}
\end{aligned} \tag{61}$$

Further, an approach based on Cauchy's residue theorem is employed for calculating analytically the integral of Eq. (59); see also [25] for more details. Specifically, consider the function

$$g_{jk}(z) = f_{jk}(z)Log(z) \tag{62}$$

where z is a complex number with a polar form $z = |z|e^{i\vartheta}$ and $\mathrm{Log}(z) = \ln|z| + i\vartheta$. Furthermore, the integral of $g_{jk}(z)$ over the boundary $\Gamma = L_1 \cup C_R \cup L_2 \cup C_r$ of the domain shown in Fig. 1 is expressed as

$$\int_\Gamma g_{jk}(z)dz = \int_{C_R} g_{jk}(z)dz + \int_{C_r} g_{jk}(z)dz + \int_{L_1} g_{jk}(z)dz + \int_{L_2} g_{jk}(z)dz \tag{63}$$

where the curves C_R, C_r, L_1 and L_2 are illustrated in Fig. 1, and are defined so that [25]

$$\begin{aligned}
&C_R : z = Re^{i\theta}, 0 \le \theta \le 2\pi;\\
&C_r : z = re^{i\theta}, 0 \le \theta \le 2\pi;\\
&L_1 : z = \omega e^{i\theta}, r \le \omega \le R \text{ and } \theta \to 0;\\
&L_2 : z = \omega e^{i(2\pi-\theta)}, r \le \omega \le R \text{ and } \theta \to 0;
\end{aligned} \tag{64}$$

Next, taking the limits $r \to 0$ and $R \to +\infty$, and accounting for the fact that the integrals over the curves C_R and C_r become zero as shown in Ref. [25], the integral of Eq. (63) takes the form

$$\lim_{\substack{r\to 0\\ R\to+\infty}} \int_\Gamma g_{jk}(z)dz = -2\pi i \int_0^{+\infty} f_{jk}(s)ds \tag{65}$$

Applying Cauchy's residue theorem to Eq. (65), and considering Eq. (59), yields [25].

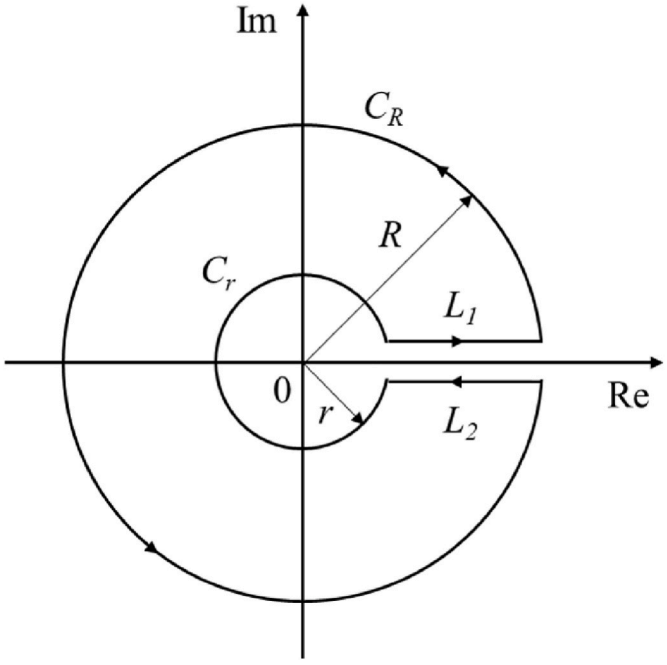

Fig. 1. Complex domain of integration.

$$I_{jk} = -\frac{b}{m^2}\sum_{l=1}^{N}\text{Res}\left[f_{jk}(z)\text{Log}(z), s_l\right] \tag{66}$$

where

$$\text{Res}\left[f_{jk}(z)\text{Log}(z), s_l\right] = \lim_{z\to s_l}(z-s_l)f_{jk}(z)\text{Log}(z) \tag{67}$$

Hence, substituting Eq. (66) into Eq. (55), the oscillator stationary response variance is given by the closed-form analytical expression

$$\sigma_x^2 = \frac{b(\rho A c_D \sigma_v)^2 d_v L_v \bar{v}}{2\pi m^2}\sum_{j=1}^{5}\sum_{k=1}^{5}\psi_{1j}^{*}\psi_{1k}\varepsilon_{1j}^{*}\varepsilon_{1k}\sum_{l=1}^{N}\text{Res}\left[f_{jk}(z)\text{Log}(z), s_l\right] \tag{68}$$

5. Numerical application

In this section a numerical application of the filter approximations is presented for demonstrating the advantages of the herein-developed filter-based modeling framework. Specifically, first, the filter parameters, both for the integer- and the fractional-order cases, are determined based on a standard least-squares optimization scheme (e.g., Ref. [42]). Next, the accuracy degree of the filter approximations for determining oscillator response statistics is assessed by comparisons both with the exact result obtained by integrating numerically Eq. (8) in conjunction with the original filter of Eq. (2), and with pertinent MCS data (10,000 realizations). The parameter values used are $\sigma_v = 1$ m/s, and $L_v = 27.7$ m, $\bar{v} = 16.01$ m/s according to Ref. [52].

5.1. Filter parameters optimization

To determine the filter parameters, a standard least-squares optimization scheme is employed (e.g., Ref. [42]) for minimizing the error in the frequency domain between the original PSD of Eq. (2) and the filter approximation of Eq. (13). Table 1 shows the computed values of the parameters p, q and r, both for the integer-order ($\beta = 1$) and the fractional-order ($\beta = 5/6$) cases. In passing, note that, as anticipated by the form of Eq. (13), the first optimization attempt yielded an estimate for r that was approximately equal to 1. Thus, r was set equal to 1, and the optimization was repeated for identifying the free variables p and q.

The two filter approximations are plotted in Fig. 2 and compared with the original PSD. It is seen that, considering the same number of unknown parameters in the optimization scheme (i.e., p, q and r), the fractional-order filter exhibits a higher degree of accuracy in approximating the original PSD compared to the integer-order filter. This is particularly true for the relatively high frequency range, where the integer-order filter fails to capture satisfactorily the characteristics of the original PSD; see Fig. 2b. Note that, alternatively, a cascade of integer-order filters can be used that can yield, potentially, enhanced accuracy (e.g., Ref. [28]). However, this translates into some additional computational effort due to the increased number of unknown parameters to be identified. In passing, note that the stability both of the integer- and of the fractional-order filters is demonstrated in the Appendix based on the standard and on the extended Ruth-Hurwitz criteria, respectively [44].

5.2. Oscillator response variance

For the integer-order filter ($\beta = 1$), Eq. (33) is used for the oscillator stationary response variance. For the fractional-order filter ($\beta = 5/6$), Eq. (68) is utilized, which requires, first, an eigenvalue analysis of matrix **D**. In this regard, numerical solution of the corresponding characteristic polynomial of Eq. (49) yields the 12 eigenvalues plotted in Fig. 3. Note that based on the optimal parameter values shown in Table 1, the coefficient multiplying λ^{12} in Eq. (50) is equal to $\frac{p}{q}\left(d_v\frac{L_v}{\bar{v}}\right)^{7/6} = 0.0185 \ll 1$. Thus, according to the rationale presented in section 4.2, the approximate characteristic polynomial of Eq. (51) is considered, and solved analytically yielding the eigenvalues of Eqs. (52)–(54). These are also plotted in Fig. 3, where it is seen that they practically coincide with the corresponding numerical estimates.

Next, Eq. (46) is used for determining the excitation PSD $S_v(\omega)$. This is done both by employing the complete set of $n = 12$ eigenvalues calculated by solving numerically the characteristic polynomial of Eq. (49), and by utilizing only $n = 5$ terms in Eq. (46) corresponding to the approximate analytical expressions of Eqs. (52)–(54). Comparisons in Fig. 4 with the original PSD of Eq. (2) show that the approximation of Eq. (46) with $n = 5$ terms based on Eqs. (52)–(54) yields a quite high degree of accuracy. In fact, the PSD estimates based on Eq. (46) using $n = 12$ and $n = 5$ coincide, practically, with minor differences observed in the relatively high frequency range. Thus, in the following, the approximation of Eq. (46) is used with $n = 5$ based on Eqs. (52)–(54).

Further, the accuracy degree of the filter approximations is assessed with respect to determining the oscillator response PSD. In this regard, the exact response PSD given by Eq. (6) in conjunction with the original excitation of Eq. (2) is compared, for the integer-order filter ($\beta = 1$), with results obtained by Eq. (14) in conjunction with Eq. (18), and for the fractional-order filter ($\beta = 5/6$), with results obtained by Eq. (48) in conjunction with $n = 5$ and Eqs. (52)–(54). This is done for two representative sets of values for the oscillator parameters, i.e., a) $\omega_0 = \pi/5$ rad/s and $\xi = 5\%$; and b) $\omega_0 = 2\pi$ rad/s and $\xi = 0.2\%$. Fig. 5 corresponds to case a), where it is shown that the fractional-order filter exhibits excellent accuracy in determining the response PSD. Note, however, that also the integer-order filter approximation succeeds in capturing, reasonably well, the salient characteristics of the response PSD. This is expected since the frequency response function of the oscillator in case a) corresponds to a frequency domain where, as shown in Fig. 2, the approximation accuracy of the integer-order filter is quite satisfactory. In contrast, regarding case b) shown in Fig. 6, the integer-order filter underestimates significantly the resonance peak of the response PSD. This is due to the fact that the oscillator frequency response function corresponds to a relatively higher frequency range where the integer-order filter exhibits a poor degree of accuracy as shown in Fig. 2.

Next, representatively, for the oscillator with parameter values $\omega_0 = \pi/5$ and $\xi = 5\%$, the stationary response variances, estimated based on Eq. (33) for the integer-order filter and on Eq. (68) for the fractional-order filter, are plotted in Fig. 7. Comparisons both with the exact result obtained by integrating numerically Eq. (8) in conjunction with the original filter of Eq. (2), and with MCS-based estimates (10,000 realizations), demonstrate a quite high degree of accuracy for the fractional-order filter approximation. For the MCS analyses, the spectral representation approach [10] has been employed for producing realizations compatible with the excitation PSD, whereas a standard 4th-order Runge-Kutta integration scheme [54] has been used for solving numerically Eq. (3). Further, as anticipated based on Fig. 5, the variance estimate obtained by relying on the integer-order filter approximation underestimates the MCS-based result. Nevertheless, it can be argued that it exhibits reasonable accuracy to be used for preliminary analysis and design purposes. More importantly, it is emphasized that the analytical evaluation of the random vibration integral of Eq. (8) via Eq. (33) is exact, and the only source of error relates to the approximation of the input excitation via Eq. (17). In this regard, note that the approximation degree can be controlled by the analyst by considering, for instance, higher-order filter representations of the input excitation (e.g., Ref. [28]). In contrast, this is not the case with

Table 1
Optimal parameters for the filter approximations of the excitation PSD.

Filter approximation	p	q	r
Integer-order ($\boldsymbol{\beta = 1}$)	$3.0782\cdot10^{-10}$	0.3251	1
Fractional-order ($\boldsymbol{\beta = 5/6}$)	$3.5776\cdot10^{-4}$	0.3447	1

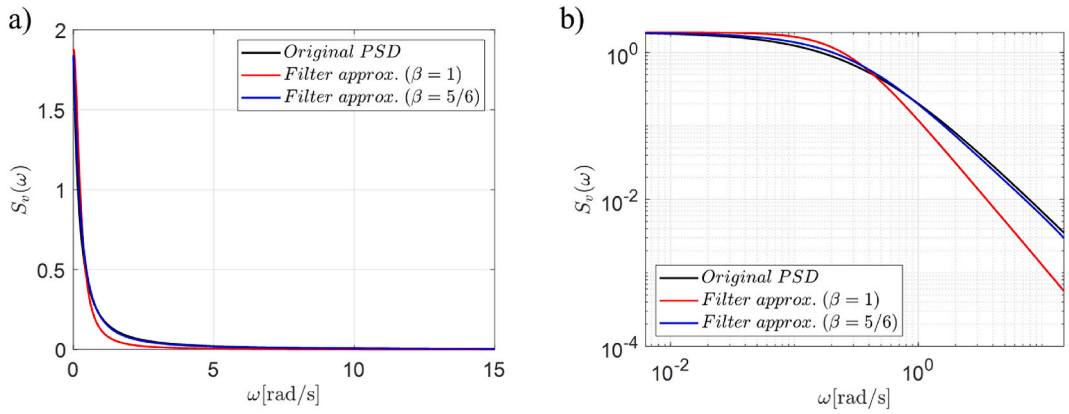

Fig. 2. Integer-order ($\beta = 1$) and fractional-order ($\beta = 5/6$) filter approximations of the excitation PSD; comparisons with the original PSD: a) linear scale, and b) logarithmic scale.

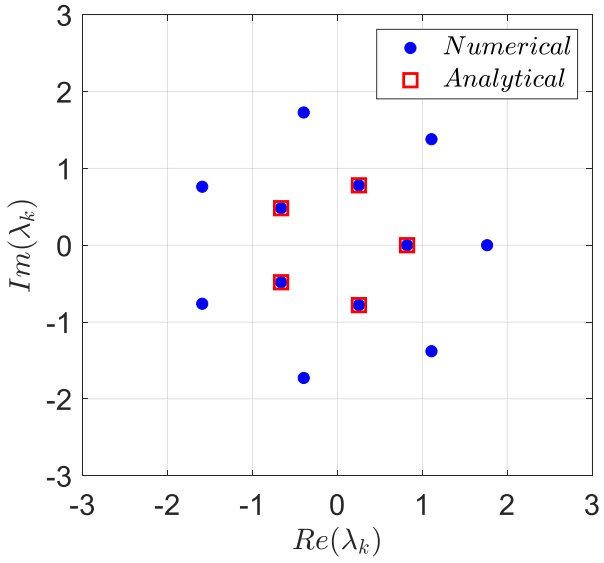

Fig. 3. Eigenvalues of matrix **D** of Eq. (39); comparisons between numerical calculation (blue) and approximate analytical estimates (red). (For interpretation of the references to colour in this figure legend, the reader is referred to the Web version of this article.)

alternative approaches embedded in relevant design codes that rely on quite strong assumptions and on rather crude simplifications for computing approximately the random vibration integral of Eq. (8) (e.g., Refs. [41,51]).

6. Concluding remarks

In this paper, a fractional-order filter approximation has been developed for the quite popular wind turbulence model proposed in Ref. [38]. Specifically, it has been shown that, considering the same number of unknown filter parameters in the associated optimization problem, the herein-developed fractional-order filter with derivative elements of rational order yields enhanced accuracy compared to a related integer-order filter. Notably, the latter can be construed as a limiting case of the former.

Further, it has been shown that the fractional-order filter approximation of the excitation PSD enables the analytical calculation of relevant random vibration integrals, at practically zero computational cost, for determining statistical moments corresponding to the response of linear structural systems. This has been done by employing a complex modal analysis treatment of the filter state-variable equations, and by relying on Cauchy's residue theorem. Comparisons both with the exact result, obtained by integrating numerically in the frequency domain the response PSD based on the original excitation model, and with pertinent MCS data have demonstrated a quite high degree of accuracy.

Furthermore, it is emphasized that the analytical calculation, achieved herein, of the random vibration integral of Eq. (8) is exact, and the only source of error relates to the approximation of the input excitation.

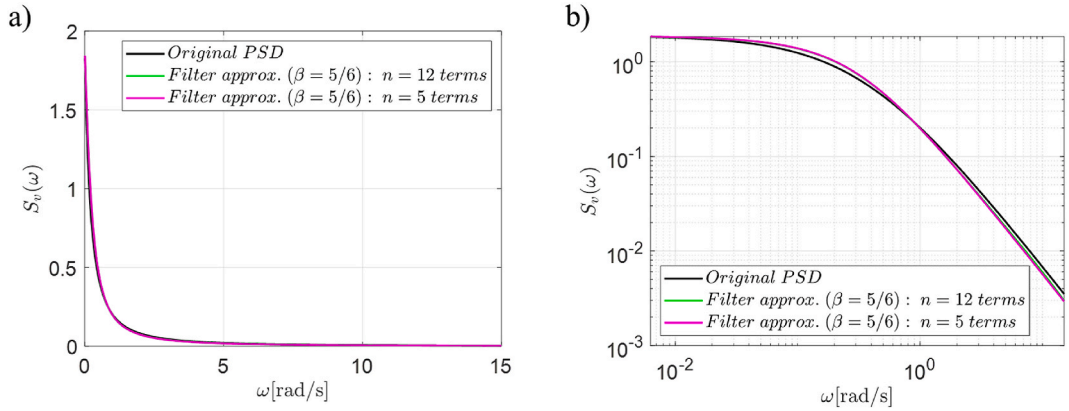

Fig. 4. Fractional-order ($\beta = 5/6$) filter approximation of the excitation PSD; comparisons between the original PSD, Eq. (46) using the numerically calculated complete set of $n = 12$ eigenvalues, and truncated Eq. (46) using $n = 5$ terms based on the approximate analytical expressions of Eqs. (52)–(54): a) linear scale, and b) logarithmic scale.

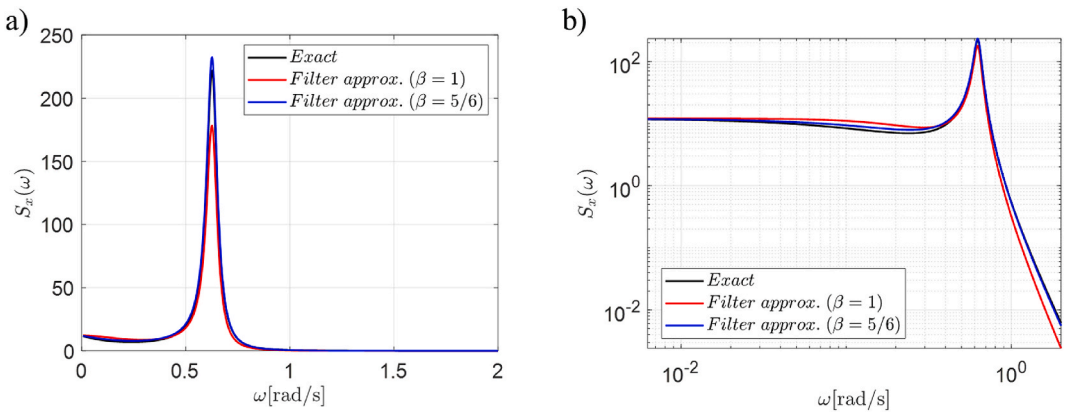

Fig. 5. Response PSD of a linear oscillator with parameter values $\omega_0 = \pi/5$ and $\xi = 5\%$; comparisons between the integer-order ($\beta = 1$) filter approximation, the fractional-order ($\beta = 5/6$) filter approximation, and the exact result: a) linear scale, and b) logarithmic scale.

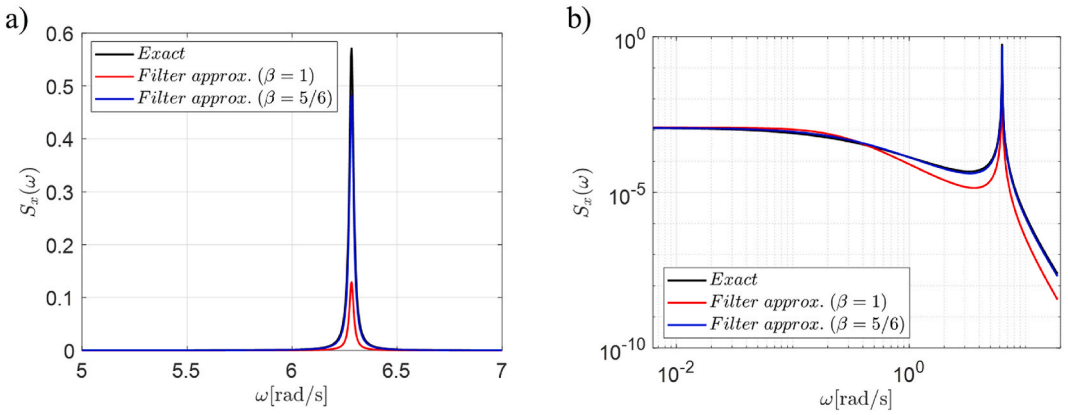

Fig. 6. Response PSD of a linear oscillator with parameter values $\omega_0 = 2\pi$ and $= 0.2\%$; comparisons between the integer-order ($\beta = 1$) filter approximation, the fractional-order ($\beta = 5/6$) filter approximation, and the exact result: a) linear scale, and b) logarithmic scale.

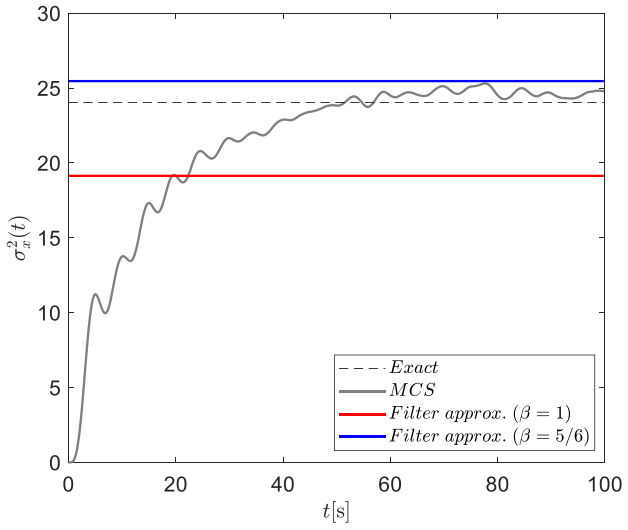

Fig. 7. Response displacement variance of a linear oscillator with parameter values $\omega_0 = \pi/5$ and $\xi = 5\%$; comparisons between the integer-order ($\beta = 1$) filter approximation, the fractional-order ($\beta = 5/6$) filter approximation, the exact result obtained by numerical integration in the frequency domain, and MCS-based estimates (10,000 realizations).

In this regard, note that the approximation degree can be controlled by the analyst by considering, for example, higher-order filter representations of the input turbulence model. This is a significant advantage of the technique compared to alternative approaches in the literature that have been adopted by relevant design codes [51], and rely on quite strong assumptions and on rather crude simplifications for computing approximately the random vibration integral of Eq. (8).

Lastly, considering the fact that the cost associated with the numerical calculation of response moments of higher-dimensional systems becomes increasingly significant, the extension of the technique to account for MDOF structural systems and excitation PSD matrices is identified as a topic of future work. Also, relying on recent work in Ref. [55] can lead, perhaps, to the generalization of the technique to treat systems endowed with fractional derivative elements, and to determine not only the stationary but also the non-stationary stochastic response.

CRediT authorship contribution statement

Luca Roncallo: Writing – review & editing, Writing – original draft, Visualization, Validation, Software, Methodology, Investigation, Funding acquisition, Formal analysis, Data curation, Conceptualization. **Ilias Mavromatis:** Writing – review & editing, Visualization, Software, Resources, Methodology, Formal analysis, Data curation, Conceptualization. **Ioannis A. Kougioumtzoglou:** Writing – review & editing, Supervision, Methodology, Formal analysis, Conceptualization. **Federica Tubino:** Writing – review & editing, Supervision, Methodology, Formal analysis, Conceptualization.

Declaration of competing interest

The authors declare that they have no known competing financial interests or personal relationships that could have appeared to influence the work reported in this paper.

Data availability

Data will be made available on request.

Acknowledgements

This research is funded by the European Research Council (ERC) under the European Union's Horizon 2020 research and innovation program (grant agreement No. 741273) for the project THUNDERR - Detection, simulation, modelling and loading of thunderstorm outflows to design wind-safer and cost-efficient structures - supported by an Advanced Grant 2016.

The data used for this research was recorded by the monitoring network set up as part of the European Projects Winds and Ports (grant No. B87E09000000007) and Wind, Ports and Sea (grant No. B82F13000100005), funded by the European Territorial Cooperation Objective, Cross-border program Italy-France Maritime 2007–2013.

The authors gratefully acknowledge financial support for this research by the Fulbright Research Scholar Program, which is sponsored by the U.S. – Italy Fulbright Commission. Its contents are solely the responsibility of the authors and do not necessarily represent the official views of the Fulbright Program, the Government of the United States, or the Italy Fulbright Commission.

Appendix

First, the standard Routh-Hurwitz criterion (e.g., Ref. [56]) is applied to the integer-order filter of Eq. (17). In this regard, the excitation-free equation corresponding to Eq. (17) is cast in the state-variable form

$$\dot{\mathbf{V}}(t) = \mathbf{A}\mathbf{V}(t) \tag{69}$$

where $\mathbf{V}(t) = [v(t)\ \dot{v}(t)]^T$ and

$$\mathbf{A} = \begin{bmatrix} 0 & 1 \\ -\dfrac{r}{p\left(d_v \frac{L_v}{\bar{v}}\right)^2} & -\dfrac{q}{p\left(d_v \dfrac{L_v}{\bar{v}}\right)} \end{bmatrix} \tag{70}$$

The characteristic polynomial corresponding to matrix $\mathbf{A}$ in Eq. (70) takes the form

$$P(\lambda) = \lambda^2 + a_1\lambda + a_2 = 0 \tag{71}$$

where $a_1 = \frac{q}{p\left(d_v \frac{L_v}{\bar{v}}\right)}$ and $a_2 = \frac{r}{p\left(d_v \frac{L_v}{\bar{v}}\right)^2}$.

According to the Routh-Hurwiz criterion (e.g., Ref. [56]), the system is stable if $H_1 = a_1 > 0$ and $\mathrm{Det}(H_2) > 0$ with

$$H_2 = \begin{bmatrix} a_1 & 1 \\ 0 & a_2 \end{bmatrix} \tag{72}$$

Note that $a_1 > 0$ and $a_2 > 0$, and thus, the criterion is satisfied.

Next, the extended Routh-Hurwitz criterion [44] is applied to the fractional-order filter of Eq. (19). In this regard, the corresponding to Eq. (19) excitation-free state-variable Eq. (37) becomes

$$\mathbf{I}\left({}_cD_0^{1/b}\mathbf{Z}\right)(t) + \mathbf{D}\mathbf{Z}(t) = \mathbf{0} \tag{73}$$

According to the extended Routh–Hurwitz stability criterion for fractional-order systems, the system is stable if

$$|\arg(\iota_j)| > \frac{\pi}{2b} \tag{74}$$

where ι_j are the eigenvalues of the matrix $-\mathbf{D}$.

Further, the numerically obtained eigenvalues related to $-\mathbf{D}$ are plotted in Fig. 8 in conjunction with the lower limit $\frac{\pi}{2b} = 0.2618$ on the right hand side of Eq. (74) pertaining to the phase of the eigenvalues. Clearly, as shown in Fig. 8, criterion of Eq. (74) is satisfied.

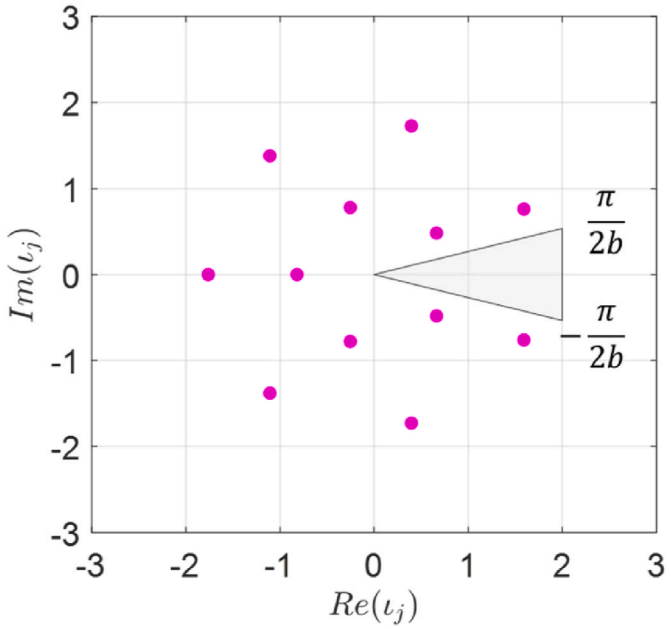

Fig. 8. Eigenvalues of matrix $-\mathbf{D}$ of Eq. (39).

References

[1] M.D. Grigoriu, Applied Non-gaussian Processes : Examples, Theory, Simulation, Linear Random Vibration, and MATLAB Solutions, 1995.
[2] E. Vanmarcke, Random fields: analysis and synthesis, World Scientific (2010).
[3] I.A. Kougioumtzoglou, I. Petromichelakis, A.F. Psaros, Sparse representations and compressive sampling approaches in engineering mechanics: a review of theoretical concepts and diverse applications, Probabilistic Eng. Mech. 61 (2020) 103082, https://doi.org/10.1016/j.probengmech.2020.103082.
[4] Y.K. Lin, Probabilistic Theory of Structural Dynamics, McGraw-Hill, 1967.
[5] I. Elishakoff, Probabilistic Theory of Structures, 1999.
[6] J.B. Roberts, P.D. Spanos, Random Vibration and Statistical Linearization, 2003.
[7] J. Li, J. Chen, Stochastic Dynamics of Structures, John Wiley & Sons, 2009.
[8] M.D. Grigoriu, Stochastic Systems: Uncertainty Quantification and Propagation, Springer London, 2012.
[9] I. Kougioumtzoglou, A. Psaros, P.D. Spanos, Path Integrals in Stochastic Engineering Dynamics, Springer, 2024, https://doi.org/10.1007/978-3-031-57863-2.
[10] M. Shinozuka, G. Deodatis, Simulation of multi-dimensional Gaussian stochastic fields by spectral representation, Appl. Mech. Rev. 49 (1996) 29–53.
[11] P.D. Spanos, B.A. Zeldin, Monte Carlo treatment of random fields: a broad perspective, Appl. Mech. Rev. 51 (1998) 219–237, https://doi.org/10.1115/1.3098999.
[12] P.D. Spanos, Spectral moments calculation of linear system output, J. Appl. Mech. 50 (1983), https://doi.org/10.1115/1.3167169.
[13] P.D. Spanos, An approach to calculating random vibration integrals, J. Appl. Mech. 54 (1987) 409–413, https://doi.org/10.1115/1.3173028.
[14] P.D. Spanos, S.M. Miller, Hilbert transform generalization of a classical random vibration integral, J. Appl. Mech. 61 (1994) 575–581, https://doi.org/10.1115/1.2901498.
[15] P.D. Spanos, M. Beer, J. Red-Horse, Karhunen–loéve expansion of stochastic processes with a modified exponential covariance kernel, J. Eng. Mech. 133 (2007) 773–779, https://doi.org/10.1061/(ASCE)0733-9399(2007)133:7(773).
[16] R.G. Ghanem, P.D. Spanos, Stochastic Finite Elements: A Spectral Approach, Dover Publications, 2003.
[17] P.D. Spanos, M.P. Mignolet, Z-Transform modeling of P-M wave spectrum, J. Eng. Mech. 112 (1986) 745–759, https://doi.org/10.1061/(ASCE)0733-9399(1986)112:8(745).
[18] W. Chai, A. Naess, B.J. Leira, Filter models for prediction of stochastic ship roll response, Probabilistic Eng. Mech. 41 (2015) 104–114, https://doi.org/10.1016/j.probengmech.2015.06.002.
[19] A.F. Psaros, O. Brudastova, G. Malara, I.A. Kougioumtzoglou, Wiener Path Integral based response determination of nonlinear systems subject to non-white, non-Gaussian, and non-stationary stochastic excitation, J. Sound Vib. 433 (2018) 314–333, https://doi.org/10.1016/j.jsv.2018.07.013.
[20] M. Di Paola, G. Failla, A. Pirrotta, Stationary and non-stationary stochastic response of linear fractional viscoelastic systems, Probabilistic Eng. Mech. 28 (2012) 85–90, https://doi.org/10.1016/j.probengmech.2011.08.017.
[21] Y. Zhang, I.A. Kougioumtzoglou, F. Kong, A Wiener path integral technique for determining the stochastic response of nonlinear oscillators with fractional derivative elements: a constrained variational formulation with free boundaries, Probabilistic Eng. Mech. 71 (2023) 103410, https://doi.org/10.1016/j.probengmech.2022.103410.
[22] A. Sreekumar, I. Kougioumtzoglou, S.P. Triantafyllou, Filter approximations for random vibroacoustics of rigid porous media, J. Risk Uncertain. Eng. Syst. Part B Mech. Eng (2024). In press.
[23] H.M. James, N.B. Nichols, R.S. Phillips, in: Hubert M. James, Nathaniel B. Nichols, Ralph S. Phillips (Eds.), Theory of Servomechanisms, Dover, 1965.
[24] J.K. Hammond, Evolutionary spectra in random vibrations, J. R. Stat. Soc. Ser. B. 35 (1973) 167–188.
[25] V. Artale, G. Navarra, A. Ricciardello, G. Barone, Exact closed-form fractional spectral moments for linear fractional oscillators excited by a white noise, J. Risk Uncertain. Eng. Syst. Part B Mech. Eng. 3 (2017) 1–6, https://doi.org/10.1115/1.4036700.
[26] N. Su, Z. Cao, Y. Wu, Fast frequency-domain algorithm for estimating the dynamic wind-induced response of large-span roofs based on cauchy's residue theorem, Int. J. Struct. Stab. Dyn. 18 (2018), https://doi.org/10.1142/S0219455418500372.
[27] P.D. Spanos, Y. Sun, N. Su, Advantages of filter approaches for the determination of wind-induced response of large-span roof structures, J. Eng. Mech. 143 (2017) 4017066, https://doi.org/10.1061/(ASCE)EM.1943-7889.0001261.
[28] P.D. Spanos, Filter approaches to wave kinematics approximation, Appl. Ocean Res. 8 (1986) 2–7, https://doi.org/10.1016/S0141-1187(86)80025-6.
[29] L. Roncallo, F. Tubino, Thunderstorm gust response factor: a closed-form solution, J. Wind Eng. Ind. Aerodyn. 240 (2023) 105487, https://doi.org/10.1016/j.jweia.2023.105487.
[30] D.K. Kwon, A. Kareem, Towards codification of thunderstorm/downburst using gust front factor: model-based and data-driven perspectives, Eng. Struct. 199 (2019) 109608.
[31] G. Solari, Gust buffeting .2. Dynamic alongwind response, J. Struct. Eng. 119 (1993) 383–398.
[32] G. Solari, Analytical estimation of the alongwind response of structures, J. Wind Eng. Ind. Aerodyn. 14 (1983) 467–477, https://doi.org/10.1016/0167-6105(83)90047-8.
[33] G. Solari, A. Kareem, On the formulation of ASCE7-95 gust effect factor, J. Wind Eng. Ind. Aerodyn. 77–78 (1998) 673–684, https://doi.org/10.1016/S0167-6105(98)00182-2.
[34] K. Oldham, J. Spanier, The Fractional Calculus Theory and Applications of Differentiation and Integration to Arbitrary Order, Elsevier Science, 1974.
[35] J. Sabatier, O. Agrawal, J. Tenreiro Machado, Advances in Fractional Calculus, Springer, 2007.
[36] Y.A. Rossikhin, M.V. Shitikova, Application of fractional calculus for dynamic problems of solid mechanics: novel trends and recent results, Appl. Mech. Rev. 63 (2010) 10801, https://doi.org/10.1115/1.4000563.
[37] G. Alotta, M. Di Paola, A. Pirrotta, Fractional Tajimi–Kanai model for simulating earthquake ground motion, Bull. Earthq. Eng. 12 (2014) 2495–2506, https://doi.org/10.1007/s10518-014-9615-z.
[38] G. Solari, G. Piccardo, Probabilistic 3-D turbulence modeling for gust buffeting of structures, Probabilistic Eng. Mech. 16 (2001) 73–86.

[39] A.G. Davenport, The Application of Statistical Concepts to the Wind Loading of Structures, vol. 19, ICE Proc, 1961, pp. 449–472.
[40] G. Solari, Turbulence modeling for gust loading, J. Struct. Eng. 113 (1987) 1550–1569.
[41] A.G. Davenport, Gust loading factors, J. Struct. Div. 93 (1967) 11–34.
[42] J. Nocedal, S. Wright, Numerical Optimization, Springer, New York, 2006. https://books.google.com/books?id=VbHYoSyelFcC.
[43] R.A. Roberts, C.T. Mullis, Digital Signal Processing, Addison-Wesley, 1987. https://books.google.com/books?id=GiBoQgAACAAJ.
[44] S. Bourafa, M. Abdelouahab, A. Moussaoui, On Some Extended Routh – Hurwitz Conditions for Fractional-Order Autonomous Systems of Order $\alpha \in (0, 2)$ and Their Applications to, 2020, p. 133, https://doi.org/10.1016/j.chaos.2020.109623.
[45] W. Chai, A. Naess, B. Leira, Stochastic roll response for a vessel with nonlinear damping models and steady heeling angles in random beam seas, Ocean Eng 120 (2016), https://doi.org/10.1016/j.oceaneng.2016.05.019.
[46] F.P. Pinnola, Statistical correlation of fractional oscillator response by complex spectral moments and state variable expansion, Commun. Nonlinear Sci. Numer. Simul. 39 (2016) 343–359, https://doi.org/10.1016/j.cnsns.2016.03.013.
[47] M. Di Paola, F.P. Pinnola, P.D. Spanos, Analysis of multi-degree-of-freedom systems with fractional derivative elements of rational order, in: 2014 Int. Conf. Fract. Differ. Its Appl. ICFDA, vol. 2014, 2014, pp. 23–25, https://doi.org/10.1109/ICFDA.2014.6967364.
[48] A. Pirrotta, I.A. Kougioumtzoglou, A. Di Matteo, V.C. Fragkoulis, A.A. Pantelous, C. Adam, Deterministic and random vibration of linear systems with singular parameter matrices and fractional derivative terms, J. Eng. Mech. 147 (2021) 1–12, https://doi.org/10.1061/(asce)em.1943-7889.0001937.
[49] J.F. Kelly, R.J. McGough, Approximate analytical time-domain Green's functions for the Caputo fractional wave equation, J. Acoust. Soc. Am. 140 (2016) 1039–1047, https://doi.org/10.1121/1.4960549.
[50] D. Kressner, Numerical methods for general and structured eigenvalue problems, lect, Notes Comput. Sci. Eng. 46 (2005), https://doi.org/10.1007/3-540-28502-4.
[51] CNR, Guide for the Assessment of Wind Actions and Effects on Structures–CNR-DT 214/2018, 2018.
[52] L. Roncallo, G. Solari, An evolutionary power spectral density model of thunderstorm outflows consistent with real-scale time-history records, J. Wind Eng. Ind. Aerodyn. 203 (2020).
[53] S. Zhang, G. Solari, P. De Gaetano, M. Burlando, M.P. Repetto, A refined analysis of thunderstorm outflow characteristics relevant to the wind loading of structures, Probabilistic Eng. Mech. 54 (2018) 9–24.
[54] L.F. Shampine, M.W. Reichelt, The MATLAB ODE suite, SIAM J. Sci. Comput. 18 (1997) 1–22, https://doi.org/10.1137/S1064827594276424.
[55] A. Di Matteo, P.D. Spanos, Determination of nonstationary stochastic response of linear oscillators with fractional derivative elements of rational order, J. Appl. Mech. (2023) 1–25, https://doi.org/10.1115/1.4064143.
[56] M. Gopal, Control Systems: Principles and Design, McGraw Hill, 2002.